Continuation Finite Element Simulation of Second Harmonic Generation in Photonic Crystals

Gang Bao[1,2], Zhengfu Xu[2] and Jianhua Yuan[3,*]

[1] *Department of Mathematics, Zhejiang University, Hangzhou 310027, China.*
[2] *Department of Mathematics, Michigan State University, East Lansing, MI 48824, USA.*
[3] *Department of Mathematics, Beijing University of Posts and Telecommunications, Beijing 100876, China.*

Abstract. A computational study on the enhancement of the second harmonic generation (SHG) in one-dimensional (1D) photonic crystals is presented. The mathematical model is derived from a nonlinear system of Maxwell's equations, which partly overcomes the shortcoming of some existing models based on the undepleted pump approximation. We designed an iterative scheme coupled with the finite element method which can be applied to simulate the SHG in one dimensional nonlinear photonic band gap structures in our previous work. For the case that the nonlinearity is strong which is desirable to enhance the conversion efficiency, a continuation method is introduced to ensure the convergence of the iterative procedure. The convergence of our method is fast. Numerical experiments also indicate the conversion efficiency of SHG can be significantly enhanced when the frequencies of the fundamental and the second harmonic wave are tuned at the photonic band edges. The maximum total conversion efficiency available reaches more than 50% in all the cases studied.

1 Introduction

Photonic crystals (PhCs) are artificially fabricated structures in which the index of refraction varies alternatively between high-index regions and low-index regions. Due to its

---

*Corresponding author. *Email addresses:* bao@math.msu.edu (G. Bao), zhengfu@math.msu.edu (Z. Xu), yuan_bupt@yahoo.com.cn (J. Yuan)

periodic variation of the refractive index, a photonic crystal (PhC) exhibits unusual dispersion properties and frequency intervals (i.e., bandgaps) in which propagating Bloch waves do not exist [1,2]. In recent years, nonlinear optical phenomena such as second harmonic generation (SHG) in nonlinear photonic crystals have attracted extensive interest because of the extraordinary capabilities of the photonic crystal structures in controlling the light of visible and infrared wavelengths. It is well known that photonic crystals inhibit propagation of electromagnetic waves within a range of frequencies (photonic band gap). In a number of applications, nonlinear PhC devices offer unique fundamental ways of enhancing a variety of nonlinear optics.

1D photonic band gap (PBG) structures are the modern version of the old interference filters. The structure with index fluctuation contributes to localization of wave across the interfaces of layers with different index of refraction. The nonlinear phenomena in 1D photonic band gap (PBG) structures are governed by the system of nonlinear Maxwell equations. H. Ammari and K. Hamdache have provided rigorous proofs of global existence, uniqueness, and regularity of solutions to a system of nonlinear Maxwell equations in [3]. In previous studies, it has been observed that the enhancement of SH generation in photonic crystals is attributed to the high density modes near the band edges under phase-matching conditions [4, 5]. A general and rigorous theory on SHG in nonlinear multilayered devices can be referred to S. Enoch and H. Akhouayri [6]. They have described a matrix method which can precisely represent the SHG in the depleted pump regime, as well as other nonlinear phenomena such as third-harmonic generation and stimulated Raman scattering.

Recently, an expansion based on the left-to-right (LTR) and right-to-left (RTL) linear modes in 1D nonlinear PhCs was reported in [7–9]. The method analyzes the fully nonlinear system by using a multiple scale expansion approach. Assuming the nonlinear effects should only affect the solution of the linear problem on a length scale much larger than the single element of the structure, the first-order expansion of the electric fields can be expressed as a combination of the LTR modes and RTL modes that depend only on the fast variable and can be calculated by standard matrix transfer techniques. In [8], the nonlinear differential equations of the amplitudes of LTR and RTL modes are solved by using a shooting procedure. This method is efficient in one dimension. Numerical results in [8] showed a number of surprising results. However, this method is based on LTR and RTL modes and multiple scales expansion, it is not straightforward to extend the idea to PBG structures in higher dimensions. In [10, 11], a variational approach that combined the finite element methods and the fixed-point iteration was investigated to study SHG in one dimensional nonlinear optical films, which can be extended to high dimensional structure. But the method fails to produce convergent solution since the iteration scheme may break down when the nonlinearity is very strong.

In this paper, we develop a continuation approach to the combination of finite element methods with a fixed-point iteration algorithm to ensure the convergence of the iterative procedure. We consider the SHG in 1D nonlinear photonic crystal structures in the presence of strong nonlinearity. Numerical results based on this approach indicate

that the SHG efficiency in 1D nonlinear PhCs can be significantly enhanced by applying strong incident wave.

Our approach to solve the underline nonlinear Helmholtz equation is based on the weak formulation of the fully nonlinear system. Since the method combining finite element methods and general fixed-point iteration is efficient when the nonlinearity is not so strong, we study the incremental field due to small increase of the intensity of the incident wave, assuming both fields continuously depend on the input. A new variational formulation for the increment fields is derived based on the perturbation technique. The incremental fields can be computed iteratively by the combination of finite element methods and the general fixed-point iteration algorithm. By increasing the input intensity successively, we can obtain the FF field and SH field for strong incident pump. The continuation method can accurately predict the field intensity distribution of both reflected and transmitted waves. The transmission, reflection and conversion efficiency in the case of strong incident pump for variety of PhC structures are studied. The numerical results show that the conversion efficiency of SHG can be significantly enhanced when the frequencies of the fundamental wave are located at the photonic band edges, and the maximum total conversion efficiency available reaches more than 50% in all the cases studied, regardless of the magnitude of the second order nonlinear susceptibility tensors. The method has the advantages of fast numerical convergence, successfully handling the problem of very strong pump, being easily extended to high dimensional PBG structures. The techniques described in this paper may also be extended to study other nonlinear phenomena in PhCs.

The outline of the remainder of this paper is as follows. In Section 2, we introduce the classical nonlinear model for SHG in one dimensional PhCs. The numerical method combining finite element methods and continuation fixed-point iteration algorithm is presented in Section 3. The properties of the SHG in one-dimensional photonic crystal structures, the conversion efficiency and accuracy of our method are demonstrated by numerical examples in Section 4.

2   Model for second harmonic generation

Consider a typical 1D photonic crystal with the structure denoted by $(AB)^m$, where m is the number of periods. The structure is assumed to be periodic in the x direction when $0 \leq x \leq D$. It is further assumed that the media are nonmagnetic with constant magnetic permittivity everywhere, there is no external charge or current present in the field, and the electric and magnetic fields are time harmonic, i.e.,

$$\mathbf{E} = Re\big[E(x,y,z)e^{-i\omega t}\big], \qquad \mathbf{H} = Re\big[H(x,y,z)e^{-i\omega t}\big].$$

Assuming both fundamental frequency and the second harmonic wave are in the transverse electric (TE) polarization, for the SHG, the Maxwell equations yield the following

coupled system [10]:

$$\frac{d^2 E_1}{dx^2} + k_0^2 n_1^2 E_1 = -k_0^2 \chi_1^{(2)} E_1^* E_2, \tag{2.1a}$$

$$\frac{d^2 E_2}{dx^2} + 4k_0^2 n_2^2 E_2 = -2k_0^2 \chi_2^{(2)} E_1^2, \tag{2.1b}$$

where E_1 and E_2 are two electric fields at fundamental frequency ω and second harmonic frequency 2ω respectively. E_1^* denotes the complex conjugate. $k_0 = \omega/c$ is the free space wavenumber. c is the speed of the light in vacuum. n_1 and n_2 are the linear refractive index functions at ω and 2ω respectively. $\chi_1^{(2)}$ and $\chi_2^{(2)}$ are two elements in the second order nonlinear susceptibility tensors at ω and 2ω.

The background structure is linear for $x < 0$ and $x > D$, i.e., the nonlinear PhC structure is placed between two linear media with the refractive index n_l ($x < 0$) and n_r ($x > D$), respectively. As discussed in [10] and [11], when the incident light is normally launched upon the surface of the sample along the x direction, in the region $x < 0$,

$$E_1(x) = E_I e^{i\alpha_l x} + E_{1R} e^{-i\alpha_l x}, \qquad E_2(x) = E_{2R} e^{-i\beta_l x},$$

where the incident electric field is $(0, E_I e^{i\alpha_l x}, 0)$, $\alpha_l = k_0 n_l$, $\beta_l = 2k_0 n_l$, E_{1R} and E_{2R} are the reflectivity constants, corresponding to frequencies ω and 2ω respectively. In the region $x > D$,

$$E_1(x) = E_{1T} e^{i\alpha_r x}, \qquad E_2(x) = E_{2T} e^{i\beta_r x},$$

where $\alpha_r = k_0 n_r$, $\beta_r = 2k_0 n_r$, E_{1T} and E_{2T} are the transmittance constants corresponding to frequencies ω and 2ω respectively. Since the tangential components of E_i and H_i are continuous across $x = 0$ and $x = D$, we have the boundary conditions as

$$\frac{dE_1}{dx}(0) = 2i\alpha_l E_I - i\alpha_l E_1(0), \tag{2.2a}$$

$$\frac{dE_2}{dx}(0) = -i\beta_l E_2(0), \tag{2.2b}$$

$$\frac{dE_1}{dx}(D) = i\alpha_r E_1(D), \tag{2.2c}$$

$$\frac{dE_2}{dx}(D) = i\beta_r E_2(D). \tag{2.2d}$$

Hence, we study the nonlinear phenomena in 1D PhCs by solving the nonlinear coupled Helmholtz equations (2.1a)-(2.1b) in domain $[0, D]$ with the boundary conditions (2.2a)-(2.2d). The variational formulation of the nonlinear system in nonlinear optical films was presented in [10]. Let v be a test function and multiply both sides of (2.1a)-(2.1b) by v^*, then integrate by parts with the boundary conditions (2.2a)-(2.2d). Since the usual jump

conditions at the interface between two homogeneous materials are valid, we have

$$a(E_1,v) = -2i\alpha_l E_I v^*(0) + k_0^2 \int_0^D \chi_1^{(2)} E_1^* E_2 v^* dx, \tag{2.3a}$$

$$b(E_2,v) = 2k_0^2 \int_0^D \chi_2^{(2)} E_1^2 v^* dx, \tag{2.3b}$$

where

$$a(E_1,v) = \int_0^D \left(\frac{dE_1}{dx} \frac{dv^*}{dx} - k_0^2 n_1^2 E_1 v^* \right) dx - i\alpha_l E_1(0)v^*(0) - i\alpha_r E_1(D)v^*(D),$$

$$b(E_2,v) = \int_0^D \left(\frac{dE_2}{dx} \frac{dv^*}{dx} - 4k_0^2 n_2^2 E_2 v^* \right) dx - i\beta_l E_2(0)v^*(0) - i\beta_r E_2(D)v^*(D).$$

It is expected to obtain high SHG efficiency in a nonlinear photonic crystal structure. Here, the conversion efficiency is measured by the ratio of the output energy at 2ω over the input energy of pump wave. For the 1D photonic crystal structures, we can define the incoming energy $e_{in} = k_0 n_l |E_I|^2$, when the incident electric field is $(0, E_I e^{ik_0 n_l x}, 0)$. The total outgoing energy will escape from four channels, which means

$$e_{out} = e_{2\omega}^+ + e_{2\omega}^- + e_\omega^+ + e_\omega^-,$$

where

$$e_{2\omega}^+ = k_0 n_r |E_{2T}|^2, \quad e_{2\omega}^- = k_0 n_r |E_{2R}|^2; \quad e_\omega^+ = k_0 n_l |E_{1T}|^2, \quad e_{2\omega}^- = k_0 n_l |E_{1R}|^2.$$

The forward SH conversion efficiency η_{SH}^+ and the backward SH conversion efficiency η_{SH}^- are defined by

$$\eta_{SH}^+ = \frac{e_{2\omega}^+}{e_{in}} = \frac{n_r |E_{2T}|^2}{n_l |E_I|^2}, \qquad \eta_{SH}^- = \frac{e_{2\omega}^-}{e_{in}} = \frac{n_r |E_{2R}|^2}{n_l |E_I|^2}.$$

The transmitted and reflected fundamental frequency (FF) field are T_{FF} and R_{FF} respectively, with

$$T_{FF} = \frac{e_\omega^+}{e_{in}} = \frac{|E_{1T}|^2}{|E_I|^2}, \qquad R_{FF} = \frac{e_\omega^-}{e_{in}} = \frac{|E_{2R}|^2}{|E_I|^2}.$$

The total energy is conserved in the sense that

$$T_{FF} + R_{FF} + \eta_{SH}^+ + \eta_{SH}^- = 1.$$

3 Continuation fixed-point iteration algorithm

On the domain $\Gamma = [0,D]$, we consider the following variational problem: find U_1 and $U_2 \in H^1(\Gamma)$, such that

$$\begin{cases} a(U_1,v) = f(U_1^* U_2, v) + h(E_I, v), & \forall v \in H^1(\Gamma), \\ b(U_2,v) = g((U_1)^2, v), & \forall v \in H^1(\Gamma), \end{cases} \tag{3.1}$$

where $a(\cdot,\cdot)$, $b(\cdot,\cdot)$,

$$f(u,v) = k_0^2 \int_0^D \chi_1^{(2)} uv^* dx, \quad h(u,v) = -2i\alpha_l uv^*(0), \quad g(u,v) = 2k_0^2 \int_0^D \chi_2^{(2)} uv^* dx$$

are bilinear: $H^1(\Gamma) \times H^1(\Gamma) \to C$. We start this section by reviewing the fixed-point iteration algorithm combined with the finite element methods to solve (3.1).

Algorithm 3.1: Fixed-Point Iteration Algorithm (FPIA)

For a given incident electric field with E_I, choose parameter $\epsilon_0 > 0$, set $j = 0$.

1. Compute $U_1^{(0)}$, which satisfies $a(U_1^{(0)}, v) = h(E_I, v)$, $\forall v \in H^1(\Gamma)$.

2. Compute $U_2^{(0)}$, which satisfies $b(U_2^{(0)}, v) = g([U_1^{(0)}]^2, v)$, $\forall v \in H^1(\Gamma)$.

3. $j = j + 1$.

4. Compute $(U_1^{(j)}, U_2^{(j)})$ by solving the following variational problem

$$\begin{cases} a(U_1^{(j)}, v) = f([U_1^{(j-1)}]^* U_2^{(j-1)}, v) + h(E_I, v), & \forall v \in H^1(\Gamma), \\ b(U_2^{(j)}, v) = g([U_1^{(j-1)}]^2, v), & \forall v \in H^1(\Gamma). \end{cases}$$

5. If $\max_{k=1,2}\{||U_k^{(j)} - U_k^{(j-1)}||/||U_k^{(j-1)}||\} < \epsilon_0$, goto Step 6; else goto Step 3.

6. Output $U_1^{(j)}$ and $U_2^{(j)}$.

The (FPIA) method for SHG in nonlinear optical films was presented in [10] and [11]. As shown by Bao and Dobson in [10], for a given E_I, the variational problem (2.3a)-(2.3b) has a unique solution E_1, E_2 when the product of $||k_0^2\chi_1^{(2)}||_{L^\infty}$ and $||2k_0^2\chi_2^{(2)}||_{L^\infty}$ is not too large. The numerical results in [10] and [11] show that the convergence of the scheme relies on the intensity of incident electric field and the second order nonlinear susceptibility tensors of the media. Moreover, when the intensity of incident electric field is very large or the product of $||k_0^2\chi_1^{(2)}||_{L^\infty}$ and $||2k_0^2\chi_2^{(2)}||_{L^\infty}$ becomes very large, the convergence of the general fixed-point iterations method may be slow, or the iteration scheme may break down, in view of Theorem 3.1 of [10].

To compute the numerical solution to the problem of SHG in the presence of strong nonlinearity (here we focus on strong incident pump), we design a continuation fixed-point iteration algorithm (CFPIA) to solve the variational problem (2.3a)-(2.3b). The basic idea of *CFPIA* is that we study the incremental field due to small increase of the intensity of the incident wave, assuming both fields continuously depend on the input. A variational formulation for the incremental fields can be derived based on the perturbation technique. The incremental fields can be computed iteratively by the combination of finite element methods and the general fixed-point iteration algorithm. By increasing the input intensity successively, we can obtain the FF field and SH field for strong incident

pump. To illustrate this idea, for instance, we consider the variational problem (3.1). Let $\delta E = E_{I,1} - E_{I,0}$ ($E_{I,1} > E_{I,0}$), and $\delta U_k = U_{k,1} - U_{k,0}$, $k = 1,2$, where $U_{1,m}$ and $U_{2,m}$ are the solution of variational problem (3.1) while the incident pump intensity is $E_{I,m}$, $m = 0,1$ respectively. The solution for $E_{I,0}$ is obtained by the combination of linear finite element method and general fixed-point iteration algorithm, the new variational formulation for the increment fields can be written as

$$\begin{cases} a(\delta U_1, v) = f(W_1, v) + h(\delta E_I, v), & \forall v \in H^1(\Gamma), \\ b(\delta U_2, v) = g(W_2, v), & \forall v \in H^1(\Gamma), \end{cases} \tag{3.2}$$

where $W_1 = \delta U_1{}^* U_{2,0} + U_{1,0}{}^* \delta U_2 + \delta U_1{}^* \delta U_2$ and $W_2 = (\delta U_1)^2 + 2U_{1,0}\delta U_1$. δU_1 and δU_2 can be solved iteratively by using the general fixed-point iterations. Therefore $U_{1,1} = U_{1,0} + \delta U_1$, $U_{2,1} = U_{2,0} + \delta U_2$. This procedure can be repeated by replacing $(U_{1,0}, U_{2,0})$ in the right-hand side of (3.2) with the computed $(U_{1,1}, U_{2,1})$. This simply means we can iteratively get the solution for lager incident field by using the continuation fixed-point iteration algorithm *CFPIA*, summarized as

Algorithm 3.2: Continuation Fixed-Point Iteration Algorithm (CFPIA)

Given the increment δE_I, and the starting $E_{I,s}$ and the ending $E_{I,e}$, choose parameter $\epsilon_0 > 0$. Set j=0.

1. Set $E_{I,0} = E_{I,s}$. Use *FPIA* with parameter ϵ_0 to obtain $U_{1,0}$, and $U_{2,0}$ satisfy the variational problem:

$$\begin{cases} a(U_{1,0}, v) = f(U_{1,0}{}^* U_{2,0}, v) + h(E_{I,0}, v), & \forall v \in H^1(\Gamma), \\ b(U_{2,0}, v) = g((U_{1,0})^2, v), & \forall v \in H^1(\Gamma). \end{cases}$$

2. $j = j + 1$ and $E_{I,j} = \delta E + E_{I,j-1}$.

3. Use *FPIA* with parameter ϵ_0 to obtain δU_1, and δU_2 satisfy the variational problem:

$$\begin{cases} a(\delta U_1, v) = f(W_1, v) + h(\delta E_I, v), & \forall v \in H^1(\Gamma), \\ b(\delta U_2, v) = g(W_2, v), & \forall v \in H^1(\Gamma), \end{cases}$$

where $W_1 = \delta U_1{}^* U_{2,0} + U_{1,0}{}^* \delta U_2 + \delta U_1{}^* \delta U_2$ and $W_2 = (\delta U_1)^2 + 2U_{1,0}\delta U_1$.

4. $U_{1,j} = U_{1,j-1} + \delta U_1$, and $U_{2,j} = U_{2,j-1} + \delta U_2$.

5. If $E_{I,j} \geq E_{I,e}$ stop; else goto Step 2.

We numerically solve the problem (2.3a)-(2.3b) to obtain the fundamental frequency field and the second harmonic filed in 1D nonlinear PhCs by following *CFPIA*, adopting the linear finite element. It is easy to compute the transmittance constants and reflectivity constants corresponding to frequencies ω and 2ω respectively. The SH conversion efficiencies and transmitted and reflected FF field can be calculated using definitions in the previous section.

4 Numerical results and discussion

Photonic crystals have brilliant geometrical properties to improve many nonlinear effects. There are two ways to enhance the SHG in nonlinear PhCs [12–17]. One is to adjust the frequencies of both the fundamental wave (FW) and the second harmonic wave (SHW) simultaneously to the photonic band edges (PBEs). The other is to introduce some defect to the nonlinear PhCs. In this paper, we consider the perfect PhCs and tune the frequencies of both FW and SHW to reach global phase matching. We expect the SH conversion efficiency to be enhanced significantly in this scenario.
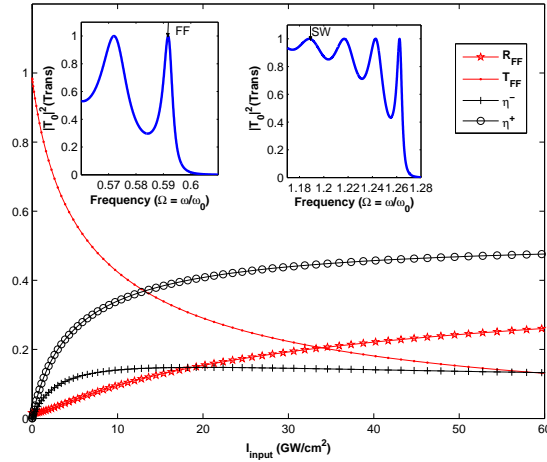
Figure 1: The backward and forward SH conversion efficiencies η^- and η^+, the transmitted and reflected FF field T_{FF} and R_{FF} for Example 1. The inserted are the linear transmittance versus the normalized frequency. The parameters for this structure are $n_1^A = 1.0$, $n_1^B = 1.42857$, $n_2^A = 1.0$, $n_2^B = 1.519$, $l_A = \lambda_0/(4n_1^A)$, $l_B = \lambda_0/(2n_1^B)$, $\Omega = 0.592$ and $\chi^{(2),B} = 120$pm/V, where $\lambda_0 = 1\mu m$.

The first example we consider is a structure composed of alternatively dielectric A-nonlinear material B layers surrounded by vacuum, M. Scalora et al. in [12]. The periodic structure has $m = 20$ layers with a lattice constant $l = l_A + l_B$, where $l_A = \lambda_0/(4n_1^A)$, and $l_B = \lambda_0/(2n_1^B)$ respectively for a reference wavelength $\lambda_0 = 1\mu m$. The refraction indices are $n_1^A = 1.0$, $n_1^B = 1.42857$, $n_2^A = 1.0$, and $n_2^B = 1.519$. Since the background medium is vacuum, we have $n_r = n_l = 1.0$. Assume that the nonlinearity is distributed uniformly throughout the PBG structure and consider the second order nonlinear susceptibility tensors $\chi^{(2),B} = 120$pm/V and the normalized frequency $\Omega = 0.592$, where $\Omega = \omega/\omega_0$, $\omega_0 = 2\pi c/\lambda_0$. We show the transmitted and reflected percentage T_{FF} and R_{FF}, the backward and forward SH conversion efficiencies η_{SH}^- and η_{SH}^+ as functions of the intensity of the incident field I_{input} in Fig. 1, where $I_{input} = \varepsilon_0 c |E_I|^2/2$. The two inserted figures are the linear transmittance versus the normalized frequency Ω. We can see the maximum total conversion efficiency $\eta_{SH}^+ + \eta_{SH}^-$ available reaches more than 50%.

The second example has the similar structure to that has been analyzed by Giuseppe
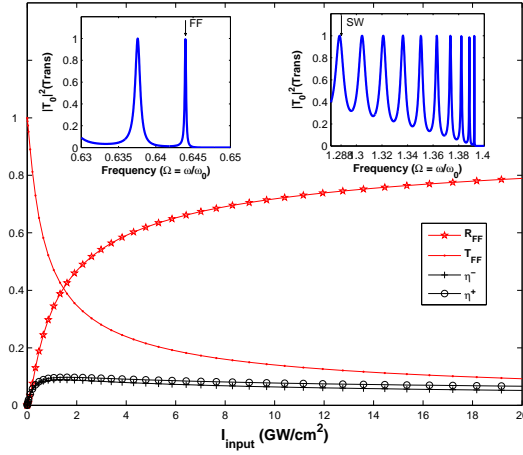
Figure 2: The backward and forward SH conversion efficiencies η^- and η^+, the transmitted and reflected FF field T_{FF} and R_{FF} for Example 2. The inserted are the linear transmittance versus the normalized frequency. The parameters for this structure are $l_A = 90$nm, $l_B = 150$nm, $n_1^A = 3.342$, $n_1^B = 1.0$, $n_2^A = 3.61$, $n_2^B = 1.0$, $\Omega = 0.64397$ and $\chi^{(2),A} = 240$pm/V.
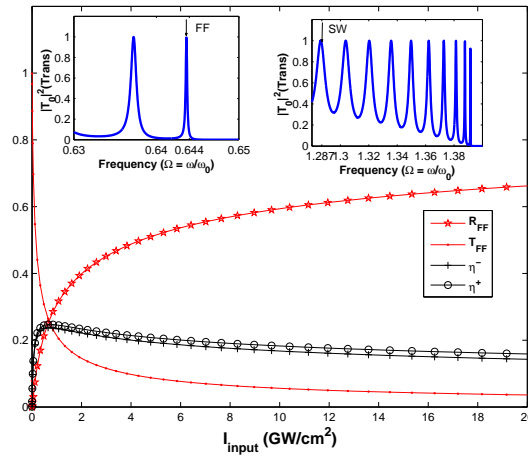
Figure 3: The backward and forward SH conversion efficiencies η^- and η^+, the transmitted and reflected FF field T_{FF} and R_{FF} for Example 3. The inserted are the linear transmittance versus the normalized frequency. The parameters for this structure are $l_A = 90$nm, $l_B = 150$nm, $n_1^A = 3.3437$, $n_1^B = 1.0$, $n_2^A = 3.61$, $n_2^B = 1.0$, $\Omega = 0.643647$ and $\chi^{(2),A} = 240$pm/V.

D. Aguanno et al. in [8], which is composed of $m = 30$ alternating layers of air and a dielectric material with $l_A = 90$nm, $l_B = 150$nm, $n_1^A = 3.342$, $n_1^B = 1.0$, $n_2^A = 3.61$, $n_2^B = 1.0$ and $n_r = n_l = 1.0$. In Fig. 2, the energy percentage of T_{FF}, R_{FF}, η_{SH}^- and η_{SH}^+ in the structure of em Example 2 versus I_{input} are show for $\Omega \approx 0.64397$, $\chi^{(2),A} = 240$pm/V. Here, the maximum total conversion efficiency available reaches approximately 20%.

It is well known the band structure and its features are strongly influenced by the number of periods, the lattice constant, and the material dispersion. For the enhance-
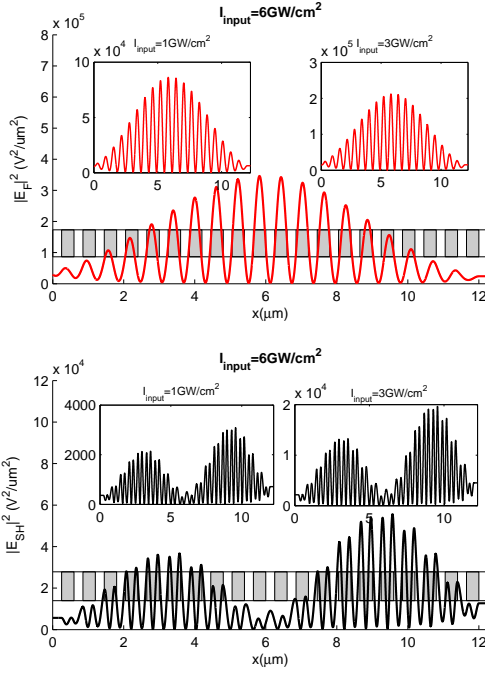
Figure 4: Absolute value squared of the FF field and of the SH field in the structure of Example 1 when $I_{input} = 6\text{GW}/\text{cm}^2$. The inserted are absolute value squared of fields when $I_{input} = 1\text{GW}/\text{cm}^2$ and $I_{input} = 3\text{GW}/\text{cm}^2$, respectively.
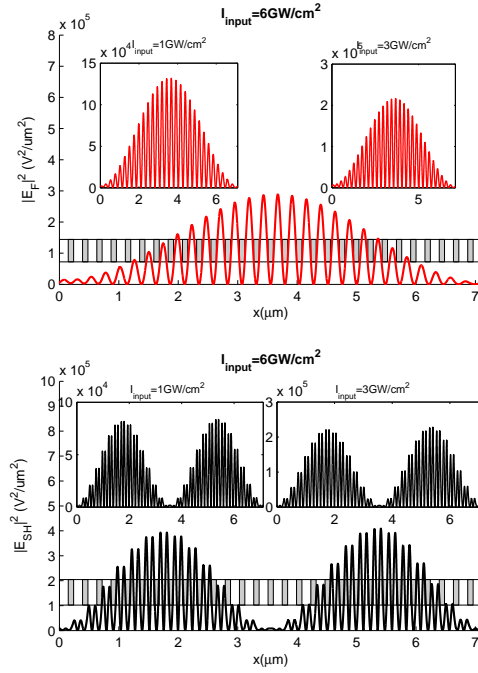
Figure 5: Absolute value squared of the FF field and of the SH field in the structure of Example 3 when $I_{input} = 6\text{GW}/\text{cm}^2$. The inserted are absolute value squared of fields when $I_{input} = 1\text{GW}/\text{cm}^2$ and $I_{input} = 3\text{GW}/\text{cm}^2$, respectively.

ment of SHG in a periodic nonlinear PhC structure, the lattice constant or the refraction indices are chosen so that both the fundamental frequency field and the second harmonic field need to be tuned sharply at the first transmission resonance near the first-order and second-order band gap transmission resonance. To illustrate this, we tune the refraction index of the dielectric material to ensure the transmission resonance. We consider the third example which has the same structure as in Example 2, but with different values of the refraction index in A-layers, $n_1^A = 3.3437$. In Fig. 3, we show the energy percentage of T_{FF}, R_{FF}, η_{SH}^- and η_{SH}^+ in the structure of Example 3. The numerical results indicate that the maximum total conversion efficiency reaches approximately 50%.

Absolute values squared of the fundamental frequency field and the second harmonic field inside the PBG structure, during the SHG process for different input intensity, are shown in Fig. 4 for the nonlinear PhC structure in Example 1, and Fig. 5 for the nonlinear PhC structure in Example 3. One may observe clearly the global phase matching between the fundamental frequency wave and second harmonic wave. Since the wavelength of second harmonic signal is half of the pump wave, there are two intensity maxima of second harmonic wave inside each high index layer, while there is a single peak for fundamental frequency wave.
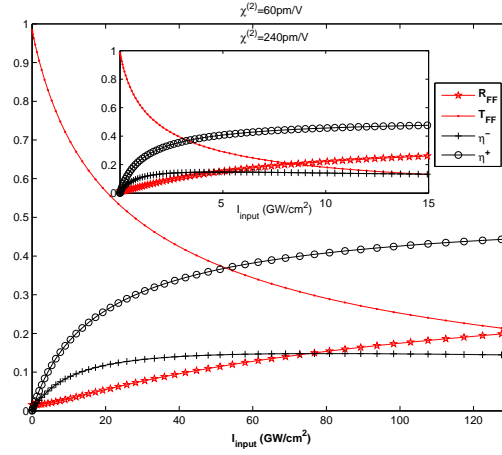
Figure 6: The SH conversion efficiencies and the transmitted and reflected FF field versus the incident fundamental frequency field I_{input} with $\chi^{(2),B} = 60$pm/V and $\chi^{(2),B} = 240$pm/V, respectively, in the structure of Example 1.
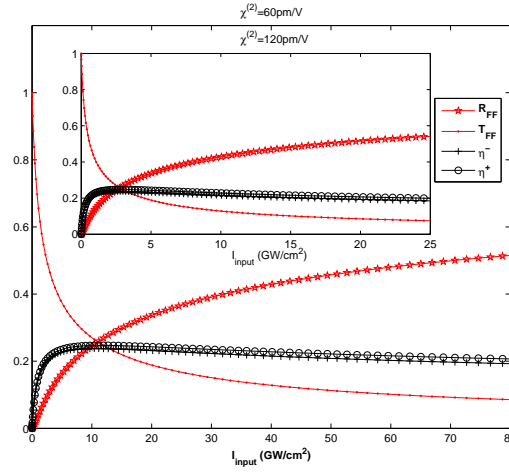
Figure 7: The SH conversion efficiencies and the transmitted and reflected FF field versus the incident fundamental frequency field I_{input} with $\chi^{(2),A} = 60$pm/V and $\chi^{(2),A} = 120$pm/V, respectively, in the structure of Example 3.

We further calculated the SH conversion efficiencies and reflected and transmitted percentage for the same structure in Example 1 and Example 3, respectively, but with different values of the nonlinear coupling coefficient. It is shown in Fig. 6 that the energy output in four channels with $\chi^{(2),B} = 60$pm/V and $\chi^{(2),B} = 240$pm/V in the structure of Example 1. In Fig. 7, the energy output is shown in four channels with $\chi^{(2),A} = 120$pm/V, and $\chi^{(2),A} = 60$pm/V in the structure of Example 3. We can draw a conclusion that the maximum total conversion efficiency available reaches more than 50% in all the cases studied, regardless of the magnitude of $\chi^{(2)}$ as long as the incident wave is strong enough.

5 Conclusions

We have presented a simple and efficient numerical method combining the finite element method and a continuation fixed-point iteration algorithm to analyze SHG in one dimensional photonic crystals. The method has the advantages of fast numerical convergence. The numerical result shows that it can successfully handle the problem of strong nonlinearity. The scheme can be conveniently extended to the two dimensional PBG structures, which will be a future project. We have also analyzed the dependence of the outgoing energy in four channels on the incident pump for the SHG in one dimensional PhCs. Our numerical results show that the conversion efficiency of SHG can be significantly enhanced by increasing the pump intensity when the frequencies of the fundamental wave and the second harmonic wave are located at the photonic band edges.

Acknowledgments

References

[1] J. D. Joannopoulos, R. D. Meade and J. N. Winn, Photonic Crystals, Molding the Flow of Light, Princeton Univ. Press, Princeton, NJ, 1995.

[2] H. Ammari, H. Kang and H. Lee, Layer Potential Techniques in Spectral Analysis, Mathematical Surveys and Monographs, Volume 153, American Mathematical Society, Providence, 2009.

[3] H. Ammari and K. Hamdache, Global existence and regularity of solutions to a system of nonlinear Maxwell equations, J. Math. Anal. Appl., 286 (2003), 51–63.

[4] A. H. Nayfeh, Introduction to Perturbation Techniques, Wiley, New York, 1993.

[5] M. Bertolott et al., Nanoscale Linear and Nonlinear Optics, Amer Inst of Physics, New York, 2001.

[6] S. Enoch and H. Akhouayri, Seond-harmonic generation in multilayered devices: theoretical tools, J. Opt. Soc. Am. B., 15 (1998), 1030–1041.

[7] G. D'Aguanno et al., Generalized coupled-mode theory for $\chi^{(2)}$ interactions in finite multilayered structures, J. Opt. Soc. Am. B., 19 (2002), 2111–2121.

[8] G. D'Aguanno and M. Centini et al., Energy exchange properties during second-harmonic generation in finite one-dimensional photonic band-gap structures with deep gratings, Phys. Rev. E., 67 (2003), 016606.

[9] M. Bertolotti, Wave interactions in photonic band structures: an overview, J. Opt. A. Pure. Appl. Opt., 8 (2006), S9–S32.

[10] G. Bao and D. C. Dobson, Second harmonic genetation in nonlinear optical films, J. Math. Phys., 35 (1994), 1622–1633.

[11] J. Yuan, Computing for second harmonic generation in one-dimensional nonlinear photonic crystals, Opt. Commun., 282(13) (2009), 2628–2633.

[12] M. Scalora and M. J. Bloemer et al., Pulsed second-harmonic generation in nonlinear, one-dimensional, periodic structures, Phys. Rev. A., 56 (1997), 3166–3174.

[13] M. Centini and M. Scalora et al., Dispersive properties of one-dimensional photonic band gap structures for second harmonic generation, J. Opt. A. Pure. Appl. Opt., 2 (2000), 121–126.

[14] H. Cao, D. B. Hall, J. M. Torkelson and C.-Q. Cao. Large enhancement of second harmonic generation in polymer films by microcavities, Appl. Phys. Lett., 76 (2000), 538–540.

[15] B. Shi, Z. M. Jiang and X. Wang, Defective photonic crystals with greatly enhanced second-harmonic generation, Opt. Lett., 26 (2001), 1194–1196.

[16] M. Centini and G. D'Aguanno et al., Non-phase-matched enhancement of second-harmonic generation in multilayer nonlinear structures with internal reflections, Opt. Lett., 29 (2004), 1924–1926.

[17] F. Ren and R. Li et al., Giant enhancement of second harmonic generation in a finite photonic crystal with a single defect and dual-localized modes, Phys. Rev. B., 70 (2004), 245109.